X-RAY SPECTROMETRY
X-Ray Spectrom. 2008; **37**: 450–457
Published online 9 May 2008 in Wiley InterScience
(www.interscience.wiley.com) DOI: 10.1002/xrs.1074

Applications of a new portable (micro) XRF instrument having low-Z elements determination capability in the field of works of art

K. Uhlir,[1]* M. Griesser,[1] G. Buzanich,[2] P. Wobrauschek,[2] C. Streli,[2] D. Wegrzynek,[3,4] A. Markowicz[3,4] and E. Chinea-Cano[3]

[1] Conservation Science Department, Kunsthistorisches Museum, Burgring 5, A-1010 Vienna, Austria
[2] Atomic Institute (ATI), Vienna University of Technology, Stadionallee 2, A-1020 Vienna, Austria
[3] Agency's Laboratories Seibersdorf, International Atomic Energy Agency (IAEA), Reaktorstrasse 1, A-2444 Seibersdorf, Austria
[4] Faculty of Physics and Applied Computer Science, AGH University of Science and Technology, Al. Mickiewicza 30, 30-059 Krakow, Poland

Received 30 January 2008; Accepted 21 March 2008

X-ray fluorescence analysis (XRF) is a powerful tool for nondestructive analysis of chemical elements present in art and archeological material. Nevertheless, investigations of objects possessing a glassy matrix still offer some problems using XRF because of the absorption in air of the low-energy characteristic fluorescence radiation of light elements. With the design of a XRF instrument equipped with a vacuum chamber housing both, the x-ray optics and the detector snout inside, a new attempt to solve this problem was made. The Conservation Science Department of the Kunsthistorisches Museum Vienna (KHM) had the opportunity to test this instrument on different objects of art. An overview of some results from these measurements, together with a short discussion of the experiences gained during the investigations, is presented in this article. Copyright © 2008 John Wiley & Sons, Ltd.

INTRODUCTION

At the laboratories of the International Atomic Energy Agency (IAEA) in Seibersdorf, Austria, a portable (μ-) x-ray fluorescence (XRF) instrument was built for the use in the field of analysis of art and archeological material. Several instruments like this have been built in the past years,[1–31] all showing problems in the detection of low-Z elements down to sodium. This is the case, because the lower the energy of the x-rays, the more absorption takes place in air. This is true for both pathways, the excitation radiation from the x-ray tube as well as for the characteristic radiation emitted from the sample. Some attempts to solve this problem have been made by using a helium flush in the radiation pathways.[1,32] Thus, results could be improved, but still there is potential for further improvement.

EXPERIMENTAL

To break new ground for the detection of low-Z elements down to sodium, the original portable XRF instrument constructed at the IAEA was redesigned with a vacuum chamber, constructed in cooperation with the Atomic Institute (ATI) of the Austrian Universities[33–35] (Fig. 1). In contrast to other instruments of this kind, the compact vacuum chamber can be evacuated to the 0.1 mbar level, and is designed to house the x-ray beam optics and the detector snout. Through a Kapton®[36,37] window of 7.5 μm thickness, the primary x-ray beam of the spectrometer can be focused on the investigated spot at about 1–2 mm distance outside of the chamber (Fig. 2). This minimizes the absorption losses of the excitation and x-ray fluorescence radiation. Two laser beams are used for positioning the chamber of the spectrometer *vs* an object under study (Fig. 3). A 50-W low-power palladium (Pd) anode x-ray tube operating up to 50 kV and 1 mA with a point focus of 400 μm is used as the excitation source. In particular the Pd L-line series with an energy around 3 keV, which is transmitted effectively through the 75-μm-thin Be window of the tube, is perfectly suited to excite the interesting light elements from Na to Cl. A polycapillary lens producing a spot size of about 40 μm, or a collimator with 1 mm inner diameter, can be used alternatively for focusing or collimation of the primary beam. The fluorescence radiation is collected by a silicon (Si) drift detector with an active area of 10 mm^2, and an 8 μm beryllium (Be) entrance window.

To proof the quality of the detection of the sodium signal, a pellet of NaCl was measured. The spectrum obtained for a measurement of 60 s is shown in Fig. 4, where sodium is clearly detectable.

For the determination of the detection limits (DL) obtained with the vacuum chamber equipped XRF instrument, a trace element reference material of the IAEA, called 'Soil 7', was analyzed. The elements that could be verified, using the measurement conditions of 1 mA, 50 kV, and a measuring time of 1500 s, as well as the calculated detection limits are listed in Table 1. For the calculation of the DLs, the following formula was used:

$$DL = \frac{3.\sqrt{N_B}}{N_N}.m \quad (1)$$

*Correspondence to: K. Uhlir, Conservation Science Department, Kunsthistorisches Museum, Burgring 5, A-1010 Vienna, Austria.
E-mail: katharina.uhlir@khm.at

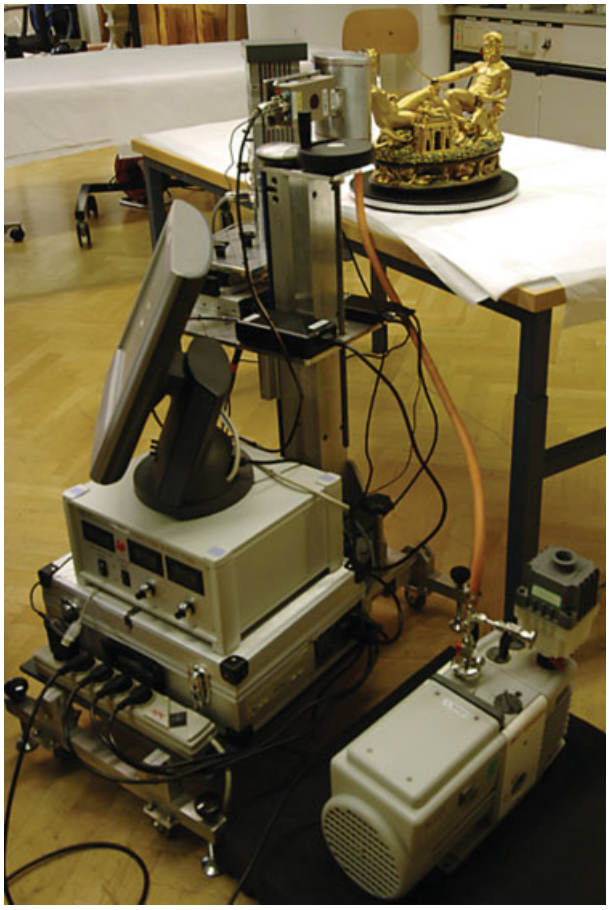

Figure 1. The vacuum chamber equipped (μ-) XRF instrument in use; positioned in front of an art object. Photo Credit: D.Calma/IAEA.

N_B . . . background signal
N_N . . . netto signal
m . . . mass of element in the sample

Although very good detection limits, especially for the light elements Al, Si and P, could be obtained, a visible bending of the chamber Kapton® window (into the vacuum chamber) occurred during the measurements, leading to an enlargement of the air path of the excitation and x-ray fluorescence radiation. Therefore, a time-dependent decrease of the fluorescence signal of the light elements was observed. After a closer investigation of this phenomenon by performing successive measurements until the intensities measured were constant in time, the problem was solved by

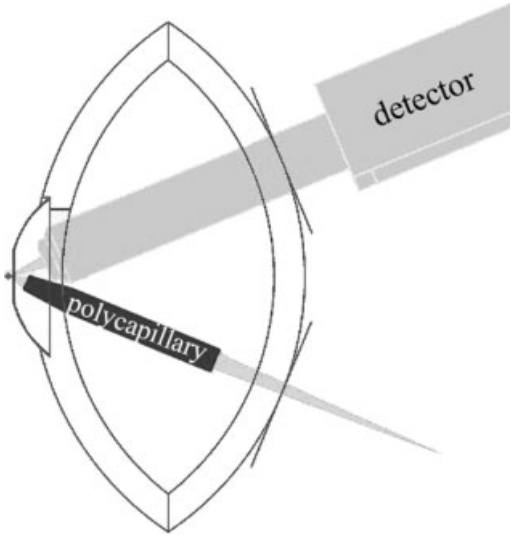

Figure 2. Geometric arrangement inside the vacuum chamber: the angle between tube and detector is 45°, the distance between detector and sample is 25 mm, the distance of the polycapillary to the sample is 15 mm. The sample is located at a distance of 1–2 mm from the Kapton® window.

Figure 3. The vacuum chamber of the (μ-) XRF instrument. The Kapton® window is located 1–2 mm from the investigated object. Photo Credit: D.Calma/IAEA.

conditioning a new mounted Kapton® window for 3 h under vacuum.

Investigating a bronze statue of a horse (modern casting of the company Venturi Arte s.r.l., Fonderia artistica, Cadriano di Granarolo E. (BO) Italia) a clear improvement in the peak intensity of the L-lines of Sn could be observed when using the evacuated instrument. Both spectra (with and without vacuum) are shown in Fig. 5. The improvement

Table 1. Detection limits calculated using the reference material 'Soil 7'

Element	Given value 'Soil 7' (mg/kg)	DL_{1500} (ppm)	Element	Given value 'Soil 7' (mg/kg)	DL_{1500} (ppm)
Al	47 000	623	V	66	28
Si	180 000	352	Cr	60	30
P	460	179	Mn	631	19
K	12 100	107	Fe	25 700	16
Ca	163 000	64	Zn	104	13
Ti	3000	26	Sr	108	37

X-RAY Spectrometry

of the line intensity using vacuum is 50%. Considering the elements Na and Cl, the improvement is even higher because of the excitation with the Pd L-lines, which show a high intensity in the excitation pathway in vacuum. Investigating pure aluminum the intensity could even be multiplied 50 times.

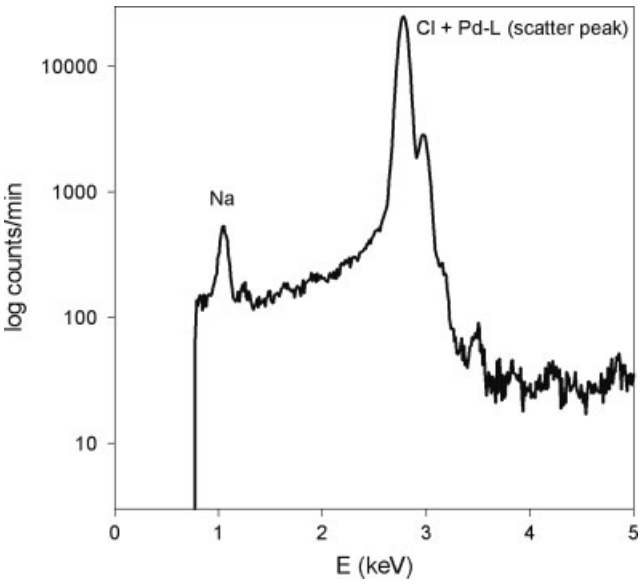

Figure 4. Spectrum of a NaCl-pellet (counts/min).

Owing to a 'Memorandum of Understanding' the Kunsthistorisches Museum Vienna (KHM) has the possibility to use the vacuum chamber-equipped instrument and was, therefore, able to test its applicability for the analysis of a variety of objects of art like Benin bronzes, ancient Egyptian objects, old master paintings, and paper objects and to perform preliminary studies for the analysis of the 15th to 17th-century enameled objects and glass items. A variety of these investigations will be presented in this paper.

The knowledge of the composition of the investigated objects is necessary either for their restoration and conservation or for art historical attributions. For the Conservation Science Department of the KHM objects consisting of metal as well as of a glassy matrix were excellent examples to apply the full capacity provided by the IAEA XRF instrument. The vacuum chamber is a big advantage, for example, for the identification of pigments containing some or exclusively light elements. Examples for this are ultramarine ($Na_{8...10}Al_6Si_6O_{24}S_{2...4}$) or Egyptian blue ($CaCuSi_4O_{10}$). Also glassy inlays, enamels, and glass objects contain light elements (Na, Mg, Al, Si, P, S, Cl). The detection of these elements is essential for the identification of the glass type and a requirement for performing quantitative analyses.

The vacuum chamber equipped (μ-) XRF instrument showed good applicability for the use at the KHM, nevertheless, some proposals for improvement could be made, which will also be discussed at the end of this article.

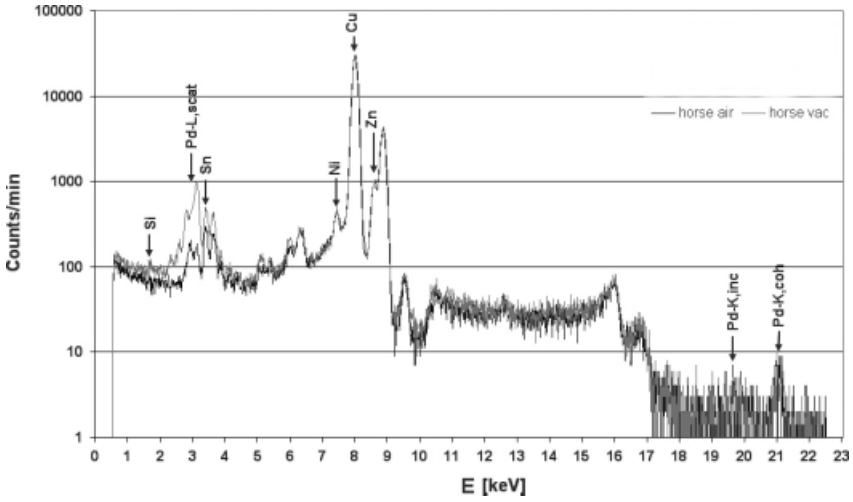

Figure 5. Spectrum of a bronze horse (modern casting of the company Venturi) with and without vacuum.

Table 2. Analyzed pigments on the Egyptian Stele, Inv. No. ÄS 5073

Investigated color	Detected elements	Identified pigment
Blue	Si, Ca, Cu	Egyptian blue ($CaO \times CuO \times 4SiO$)
Dark green	Cu	Malachite ($CuCO_3 \times Cu(OH)_2$)
Light green	Cu	Malachite ($CuCO_3 \times Cu(OH)_2$)
Red	Fe	Red ochre (Fe_2O_3)
Orange	Fe, As	Red ochre (Fe_2O_3) with orpiment or realgar
Red and blue above filling (left border in Fig. 3)	Composition varies strongly from the other areas of these colors	Later addition
Ground layer	Ca	Chalk ($CaCO_3$)
Yellow	Fe	Yellow ochre ($Fe_2O_3.nH_2O$)

DOI: 10.1002/xrs

RESULTS

Analysis of objects from the Egyptian and the Near-Eastern collection

Egyptian stele (KHM, Inv. No. ÄS 5073)

The Egyptian Stele shown in Fig. 6 can be dated to the 26th dynasty (~640 B.C.), Thebes, and is made of painted wood with a white ground layer. For restoration purposes, the pigments used for its design were investigated. The analyzed colors, the detected elements, and the identified pigments are listed in Table 2.

In this object, no complex mixing of pigments occurs and the identification had been done quite easily. Indeed, all pigments in the investigated areas were identified. The green areas contained malachite, the red areas red ochre and sometimes orpiment or realgar (As_2S_3 or As_2S_2, respectively—realgar shows a more orange color but is not distinguishable from orpiment with energy-dispersive XRF). The yellow area is made of yellow ochre, and the ground contains chalk. The pigments in the filling are completely different from the look-alike colors in the residual object, supporting the assumption that this was done later on.

The new XRF instrument was especially helpful in the analysis of Egyptian blue (Fig. 7), where high silicon intensities could be observed compared to conventionally designed portable XRF instruments. The observed impurities are partly of environmental origin.

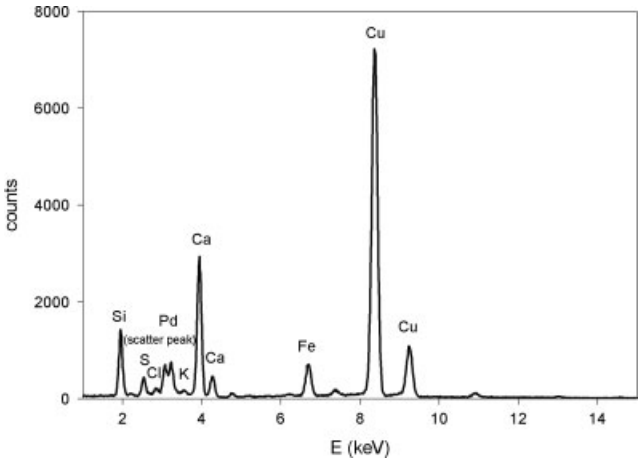

Figure 7. Spectrum of Egyptian blue.

Egyptian stucco objects (KHM, Inv. Nos. ÄS 8513, ÄS 8515, and ÄS 6154)

Several stucco objects from the Egyptian and the Near-Eastern collection have been analyzed concerning the pigments used for their decoration as well as for the identification and classification of accompanying materials, especially glass. Three examples can be given: the stucco mask ÄS 8513 (Fig. 8) from a mummy of a woman, dated to the middle of the 1st century A.D., shows a broad palette of colors: for the background orpiment or probably realgar could be identified. The blue background of the inscription field is made of Egyptian blue, and the red boarder line of this field is made of red lead. These were all very common pigments at that time.

Two other stucco masks Inv. No. ÄS 8515, from a mummy of a man with a beard, dated to the 2nd quarter of the 2nd century A.D., and Inv. No. ÄS 6154, a fragment of a face, dated between 117 and 138 A.D.,[38] have inlayed glass for the decoration of the eyes. In both cases, the iris of the eyes has been analyzed to investigate their manner of coloring. The spectrum obtained from the iris of the 'man

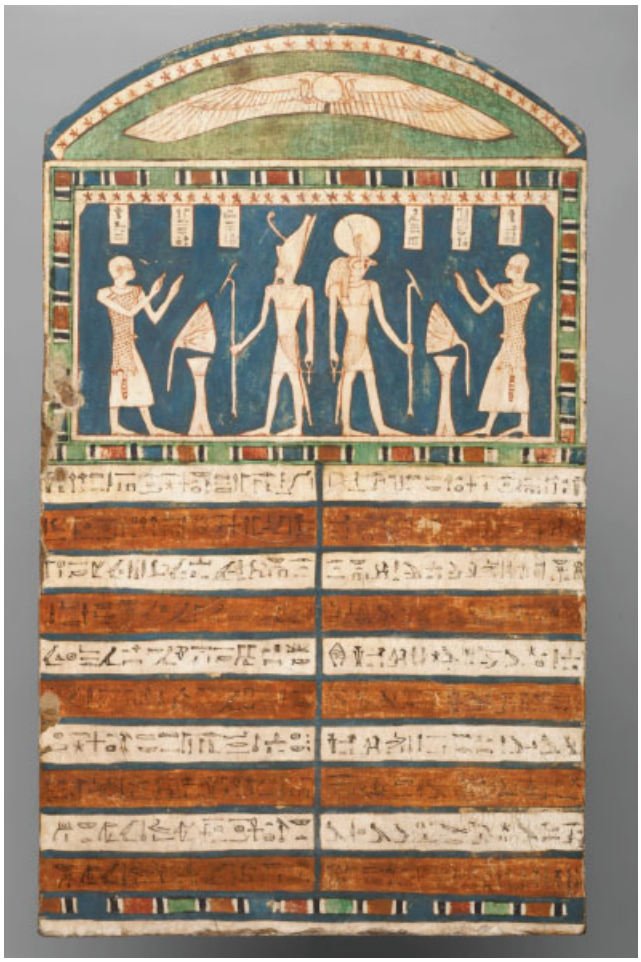

Figure 6. Egyptian stele (KHM, Inv. No. ÄS 5073), 26th dynasty, Thebes.

Figure 8. Stucco mask, KHM, Inv. No. ÄS 8513, from a mummy of a woman, dated to the middle of the 1st century A.D. Two different views are shown.

DOI: 10.1002/xrs

X-RAY Spectrometry

with beard' is shown in Fig. 9 (black line). As can be seen, the main components like silicon, calcium, and potassium can be detected very easily. Also seen are components appearing in much smaller amounts in glassy matrices like aluminum, phosphorus, and sulphur,[39,40] which are not or only barely detectable with XRF instruments operating in air. For the dark coloring of the iris, the elements manganese and iron are responsible. By contrast, the glass of the iris of the fragment of the face (Inv. No. ÄS 6154) shows no coloring additives (Fig. 9). The dark color is due to painting underneath the colorless transparent glass. A sparse but, nevertheless, detectable sodium peak can be identified, indicating a soda-lime glass, very common in the 2nd century A.D. Additionally, lead traces could be identified.

Analysis of an Oriental saddle of the Collection of Arms and Armor

The Oriental saddle of the KHM, Inv. No. C 142 is a precious object of wood covered with skin and leather, transparently painted on a dark ground (Fig. 10). From previous studies on cross sections of the paint layers using light microscopy (Fig. 11) and SEM/EDX (energy dispersive scanning electron microscopy) it could be seen that there is a white ground layer consisting of lead white. On top, a dark layer, probably from carbon black (not detectable by SEM/EDX), with an additional copper (blue or green) pigment was applied. This is followed by several organic layers, probably resin-containing, because of their fluorescence under UV-light. Above these layers, the decoration, which was analyzed using XRF, starts. On a closer look at some imperfections of the painting, it turned out that there was a red underpainting underneath the better part of the dark layer that could be identified as minium (or red lead, Pb_3O_4).

In some areas of the background, the black looked a little bit more greenish, but after removing the varnish it became clear that there was a blue background that appeared green because of the yellowish varnish. In the XRF spectrum of this blue area, intense calcium, potassium, silicon, and aluminum peaks could be identified, indicating that the blue pigment had to be a silicate material like ultramarine or lapis lazuli (Fig. 12). Additionally, like in the residual black background, a copper pigment was present also in these areas.

Because of the detection of mercury in some red areas of the decoration cinnabar (HgS) could be identified. In these parts also some tinsel could be seen, that was identified as being made of gold.

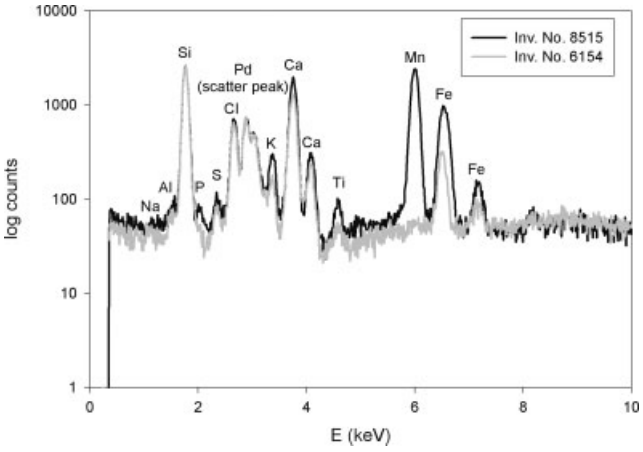

Figure 9. The spectrum of the glass inlay of the iris of the stucco mask 'man with beard' (KHM, Inv. No ÄS 8515) is shown in black. The spectrum of the glass inlay of the iris of the stucco mask 'fragment of a face' (KHM, Inv. No ÄS 6154) is shown in gray.

Figure 10. Oriental saddle (KHM, Inv. No. C 142) with details of the decoration.

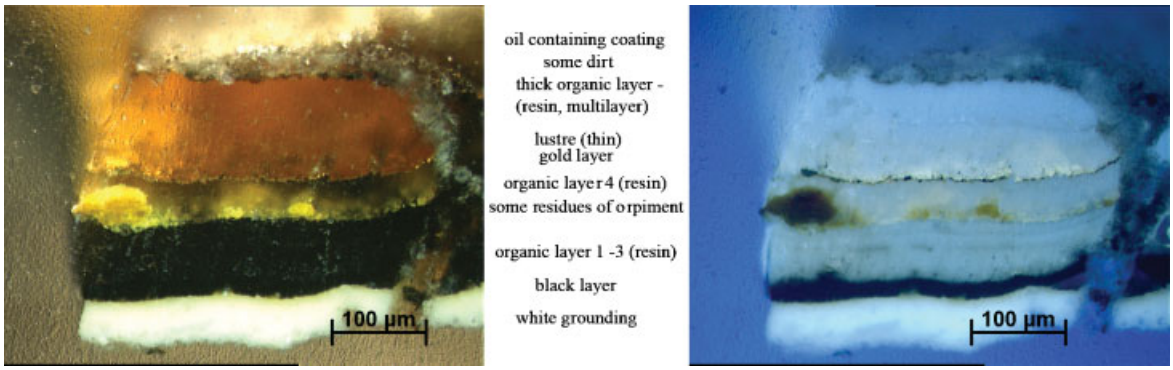

Figure 11. Cross section from the Oriental saddle (KHM, Inv. No. C 142).

DOI: 10.1002/xrs

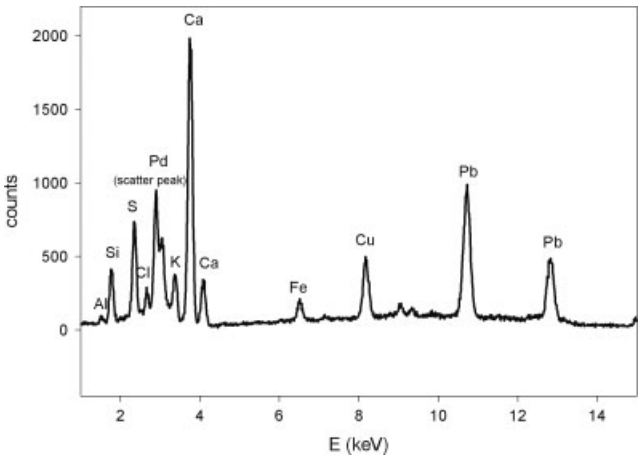

Figure 12. Spectrum of the bluish background in some areas of the decoration of the Oriental saddle (KHM, Inv. No. C 142).

Figure 13. (a) Dwarf (MVK, Inv. No. 64.745), (b) head (MVK, Inv. No. 98.160).

Analysis of Benin bronzes of the museum of ethnology (Museum für Völkerkunde (MVK))

Owing to intense trade between the kingdom of Benin and the Portuguese, French, Dutch, and the English, an exchange of goods with these nations took place from the 15th century A.D. Therefore, the people of Benin came to possess bronze very early and nowadays their bronze sculptures are of inestimable value.

Altogether 21 pieces of Benin bronzes were analyzed to characterize their composition. Again XRF was used for the analyses, but due to the patina present on the objects a preparation of the investigated areas was necessary before the analysis. As far as possible, these areas were chosen from a hidden part, like the bottom side that is often mounted on an additional plate. For the preparation, a small area (about 3×3 mm) was ground to remove the patina.

The results concerning the tin (the intensity of the investigated L-line could be improved using the vacuum chamber-equipped XRF instrument) and zinc proportion of the bronzes show a tendency: early bronzes contain a higher amount of tin, nearly equal to the proportion of zinc, whereas in later pieces the tin virtually disappears and the zinc content rises to approximately 15%. Two examples can be given: a dwarf , MVK, Inv. No. 64.735 (Fig. 13(a)), is an early object dated to the 15th century, and a head, MVK, Inv. No. 98.160 (Fig. 13(b)), is a late piece dated to the 17th–18th centuries A.D. In the spectrum of the 'head' (Fig. 14) the tin peak clearly disappears and the zinc peak rises in comparison with the spectrum of the 'dwarf'.

Although there seems to be a change with time in the composition of the bronzes, the number of investigated objects is too small to give general trends. For clarification and further study of this matter, a larger number of Benin bronzes needs to be analyzed.

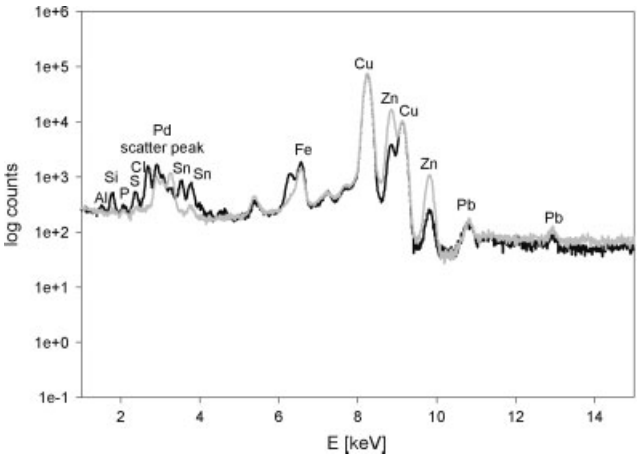

Figure 14. Spectrum of the bronzes 'dwarf' (black) and 'head' (grey).

Analysis of glass and enamel standards

The KHM, especially the Collection of Sculpture and Decorative Arts, holds a wide variety of objects made of glass or decorated with enamel. Glass and enamel, in particular, are very sensitive to environmental conditions often causing corrosion phenomena.[41] In the museum, nowadays, the storage conditions are set to minimize corrosion of these precious objects. Nevertheless, there is an urgent need for many objects to be restored and to conserve the delicate material for the future. For these projects, it is necessary to know about the composition of the glass and enamel under consideration. Therefore, some preliminary studies on glass standards have been carried out with the vacuum chamber equipped XRF instrument to outline the feasibility of the (semi-) quantitative analyses of glassy low-Z matrices.

The first step was to optimize the conditions for the analysis. It turned out that for the enhancement of x-ray lines with low energy, the polycapillary is the focusing unit of choice. The x-ray tube was set to maximum power (50 kV, 1 mA) and the measurement time to 1000 s. Although such a long measuring time was chosen, no discoloration of the investigated areas caused by the radiation dose was visible.

After the conditioning of a new Kapton® window, some glass standard reference materials (SRM) of the National Institute of Standards and Technology, (NIST SRM 610, 620, 621, 1412, 1831) and two model enamels (MDS8 and MGM2[42–44]) derived from a Deutsche Bundesstiftung

DOI: 10.1002/xrs

X-RAY Spectrometry

Umwelt (DBU) research-project,[2] were measured and then evaluated with the XRF-FP (fundamental parameter) Quantitative Analysis Software of Amptek using fundamental parameters: the method created for the evaluation consists of coefficients from five different standards (NIST 620, 1831, 1412, and the model enamels MDS8 and MGM2) and was checked by evaluating these five and the remaining two standards listed above. For comparison, some of these standard materials have also been investigated by SEM/EDX.

The following observations could be made: the evaluated concentrations of some elements of the model enamel MDS8 show some deviations from the given values, with XRF as well as with SEM/EDX. One is in the calculated concentration of chlorine, which is much less than the given value (Fig. 15). Additionally in this, standard sulphur is not detectable with XRF and shows a much smaller value than the given one (0.3% *vs* 0.9%) when investigating this model enamel with SEM/EDX. Aluminum shows a high error in the evaluation with XRF. Therefore, when the error ranges for the different elements were estimated, these elements in model enamel MDS8 were not considered. Also, the aluminum value of the NIST SRM 1412 shows a big difference between the calculated and the given value (3.6 *vs* 7.5%). This results because the coefficient of the method used is not suitable for such high values (~7.5%), indicating that the standard materials used must have concentrations as close as possible related to the material under consideration. Nevertheless, the NIST SRM 1412 does not show a composition in the enamel that can be expected during the 15th–17th centuries.

Taking into consideration the discussed irregularities in the evaluation of the SRMs and model enamels, the error that can be expected for the main glass components and the enamel during the 15th–17th centuries performing quantitative evaluation (using the vacuum chamber equipped

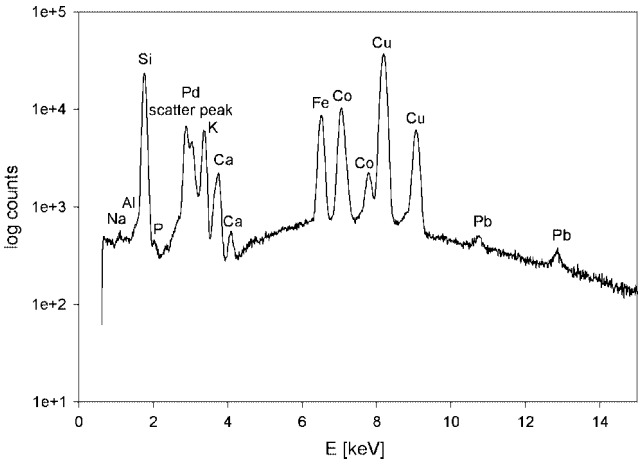

Figure 15. Spectrum of the model enamel MDS8.

[2]DBU-Projekt Nr. 09715: ''Modellhaftes Konservierungskonzept für umweltgeschädigte Emailpretiosen im Grünen Gewölbe Dresden''. The model enamels MDS8 and MGM2 were manufactured by the following project partners: Bundesanstalt für Materialforschung und -prüfung (BAM), D-12205 Berlin, Fachgruppe IV.2 (Umweltrelevante Material- und Produkteigenschaften) and Fraunhofer-Institut für Silicatforschung (ISC) in Würzburg, Außenstelle Bronnbach, D-97877 Wertheim, Kompetenzfeld für Kulturgüterschutz und Umweltmonitoring.

Table 3. Resulting error bars for specific elements measured in a glass matrix

Compound	Error bars
Na_2O	About ±25%
MgO	About ±30% for conc. >0.5%
Al_2O_3	Up to ±30% for NIST standards of soda-lime glass
SiO_2	About ±7%
K_2O	Depends highly on the concentration (±15% for conc. >2%)
CaO	About ±5%

XRF instrument and the Amptek XRF-FP software) can be estimated as shown in Table 3. Considering these relative uncertainties, it can be stated that an evaluation of the elements down to sodium is possible but the results can only be treated as semiquantitative taking into account error bars of ±30% for the light elements in the glassy matrix. This is a valuable result for archeometric interpretations.

CONCLUSIONS

The portable (μ-) XRF instrument constructed by the IAEA and equipped with a vacuum chamber for low-Z analysis by the ATI has proved very useful for the problems occurring in such a miscellaneous collection as the KHM with its affiliated institutions, the MVK (Museum für Völkerkunde—Museum of Ethnology) and ÖTM (Österreichisches Theatermuseum—Austrian Theatre Museum).

For the quantitative analysis of alloys, like bronzes, and the identification of pigments, including those that contain low-Z elements, the instrument was applied successfully. Problems only occurred with the size of the vacuum chamber, sometimes limiting the accessibility to certain parts of the objects.

The qualitative analysis of glass and enamel is possible, if the light elements are present in sufficient amounts (e.g. 10–12% for Na_2O). Nevertheless, the evaluation of these elements can only be done in a semiquantitative way because of the relative errors occurring during the investigations of the light elements. Additionally, for the setting of the coefficients in the XRF-FP software a SRM is needed that shows a very similar composition of the glassy matrix under consideration. As there are only a few SRMs available for glass analysis, this remains one of the main problems. For elements not present in these SRMs, the coefficients have to be set as an average value of the neighboring elements, provided that these elements are present in the SRM. The evaluation method using standards is necessary because of the use of the polycapillary, where the excitation profile is not known in detail. Additionally, the strong absorption of the light elements in air, increased by the bending of the Kapton® window into the vacuum chamber leads to some uncertainties in the air path length. Our trials of evaluation of glassy matrices using a nonstandard method failed.

Because of the problems described (mainly with the investigation of glass and enamel), it is planned to build a

DOI: 10.1002/xrs

new vacuum chamber equipped XRF instrument that shows some improvement:

- an innovative design of the vacuum chamber
- the application of new technology to enhance the x-ray power (up to 1.5 mA)
- the employment of advanced detector technology
- a solution to the problems concerning the bending of the Kapton® window.

With this innovative XRF instument, it is hoped that an improved quantitative analysis of glass and enamel will be possible. Additionally, this instrument will be permanently located at the KHM and will, therefore, be available for studying different problems connected to the highly valuable objects of the museum's collections.

Acknowledgements

The authors wish to thank the following departments and affiliated institutions of the KHM and their employees for their kind cooperation:

- Egyptian and Near-Eastern Collection, KHM
  Elfriede Haslauer, Irene Engelhardt
- Collection of Arms and Armour, KHM
  Christian Beaufort, Christa Angermann
- Collection of Sculpture and Decorative Arts, KHM
  Helmut Trnek, Franz Kirchweger, Helene Hanzer, Johanna Diehl
- Museum of Ethnology Vienna
  Christian Feest, Barbara Plankensteiner, Florian Rainer

Special thanks go to Rainer Richter for providing the model enamels MDS8 and MDM2 for our studies.

REFERENCES

1. Bronk H, Röhrs S, Bjeoumikhov A, Langhoff N, Schmalz J, Wedell R, Gorny HE, Herold A, Waldschläger U. *Fresenius' J. Anal. Chem.* 2001; **371**(3): 307.
2. Chiara Guazzoni Website. 2007; http://home.dei.polimi.it/longoni/xrfart/summary.htm [25 September 2007].
3. AppliTek Website. 2007; http://www.applitek.com/shownieuws.asp?language=EN&IDnr=1786 [25 September 2007].
4. Innov-X Systems Website. 2007; http://www.innov-x-sys.com/products/handheld [25 September 2007].
5. Amptek Website. 2007; http://www.amptek.com/art.html [25 September 2007].
6. Bichlmeier S, Janssens K, Heckel J, Gibson D, Hoffmann P, Ortner HM. *X-Ray Spectrom.* 2001; **30**: 8.
7. Vittiglio G, Bichlmeier S, Klinger P, Jeckel J, Fuzhong W, Vincze L, Janssens K, Engström P, Rindby A, Dietrich K, Jembrih-Simbürger D, Schreiner M, Denis D, Lakdar A, Lamotte A. *Nucl. Instrum. Methods Phys. Res., Sect. B* 2004; **213**: 693.
8. Canadian Conservation Institut (CCI) Newsletter. 2005;; **35**. http://www.cci-icc.gc.ca/publications/newsletters/news35/x-ray_e.aspx [25 September 2007].
9. Zarkadas C, Karydas AG. *Spectrochim. Acta, Part B* 2004; **59**: 1611.
10. Karydas AG, Kotzamani D, Bernard R, Barrandon JN, Zarkadas C. *Nucl. Instrum. Methods Phys. Res. B* 2004; **226**: 15.
11. Papadopoulou DN, Zachariadis GA, Anthemidis AN, Tsirliganis NC, Stratis JA. *Spectrochim. Acta, Part B* 2004; **59**: 1877.
12. Adriaens A. *Spectrochim. Acta, Part B, At. Spectrosc.* 2005; **60**: 1503.
13. Papadopoulou D, Sakalis A, Merousis N, Tsirliganis NC. *Nucl. Instrum. Methods Phys. Res. A* 2007; **580**: 743.
14. Paternoster G, Rinzivillo R, Nunziata F, Castellucci EM, Lofrumento C, Zoppi A, Felici AC, Fronterotta G, Nicolais C, Piacentini M, Sciuti S, Vendittelli M. *J. Cult. Herit.* 2005; **6**: 21.
15. Szökefalvi-Nagy Z, Demeter I, Kocsonya A, Kovács I. *Nucl. Instrum. Methods Phys. Res., Sect. B* 2004; **226**: 53.
16. Uda M, Ishizaki A, Satoh R, Okada K, Nakajima Y, Yamashita D, Ohashi K, Sakuraba Y, Shimono A, Kojima D. *Nucl. Instrum. Methods Phys. Res., Sect. B* 2005; **239**: 77.
17. Ferretti M, Cristoforetti G, Legnaioli S, Palleschi V, Salvetti A, Tognoni E, Console E, Palaia P. *Spectrochim. Acta, Part B, At. Spectrosc.* 2007; **62**: 1512.
18. Craig N, Speakman RJ, Popelka-Filcoff RS, Glascock MD, Robertson JD, Shackley MS, Aldenderfer MS. *J. Archaeol. Sci.* 2007; **34**: 2012.
19. Moioli P, Seccaroni C. *X-Ray Spectrom.* 2000; **29**: 48.
20. 15th World Conference on Nondestructive Testing Website, Roma (Italy) 15–21 October. 2000; http://www.ndt.net/article/wcndt00/papers/idn680/idn680.htm [4 January 2008].
21. Röhrs S, Stege H. *X-Ray Spectrom.* 2004; **33**: 396.
22. Jembrih-Simbürger D, Desnica V, Schreiner M, Thobois E, Singer H, Bovagnet K. *Techne—Art graphiques*. 2005; **22**: 32.
23. Hayakawa Y. *Adv. X-Ray Anal.* 2004; **47**: 36.
24. Uhlir K, Melcher M, Schreiner M. Naturwissenschaftliche Untersuchungen an antiken Gläsern aus Ephesos. In *Hanghaus 1 in Ephesos—Die Gläser*, Czura-Ruth B (ed.). Forschungen in Ephesos Bd. VIII/7: VÖAW, 2007; 231.
25. Hayakawa Y, Shirono S, Miura S, Matsushima T, Uchida T. *Powder Diffract.* 2007; **22/2**: 126.
26. Dussubieux L, Pinchin SE, Tsang J, Tumosa C. *Preprints of the 14th ICON-CC Triennial Meeting*, The Hague, 2, 2005; 766.
27. Janssens K. A survey of the recent use of x-ray beam methods for non-destructive investigations in the cultural heritage sector. In *Cultural Heritage Conservation and Environmental Impact Assessment by Non-destructive Testing and Micro Analysis*, van Grieken R, Janssens K (eds). A.A. Balkema Publishers: London, 2005; 265.
28. Gigante GE, Ridolfi S, Ricciardi P. Quantitative analysis of ancient metal artefacts by means of portable energy-dispersive x-ray fluorescence spectrometers: a critical review. In *Cultural Heritage Conservation and Environmental Impact Assessment by Non-destructive Testing and Micro Analysis*, van Grieken R, Janssens K (eds). A.A. Balkema Publishers: London, 2005; 1.
29. Gigante GE, Ricciardi P, Ridolfi S. *Rev. Archéomet.* 2005; **29**: 61.
30. Pappalardo G, Costa E, Marchetta C. *J. Cult. Herit.* 2004; **5/2**: 183.
31. Bandini G, Felici AC, Fronterotta G, Nicolais C, Piacentini M, Vendittelli M. *Archeometria della ceramica* 2002; **5**: 35.
32. Röhrs S. PhD theses. 2004; http://edocs.tu-berlin.de/diss/2003/roehrs_stefan.pdf [25.9.2007].
33. Wobrauschek P, Frank B, Zoeger N, Streli C, Cernohlawek N, Jokubonis C, Hoefler H. *Adv. X-Ray Anal.* 2005; **48**: 229.
34. Streli C, Marosi N, Wobrauschek P, Frank B. *RIGAKU J.* 2003; **20**(2): 25.
35. Buzanich G, Wobrauschek P, Streli C, Markowicz A, Wegrzynek D, Chinea-Cano E, Bamford S. *Spectrochimica Acta Part B*. special issue of ICXOM 2005. 2007; **62/11**: 1252.
36. Henke BL, Gullikson EM, Davis JC. *Atomic Data and Nuclear Data Tables*. 1993; **54**(2): 181.
37. homepage National Science Digital Library. http://henke.lbl.gov/optical_constants/ [4.1.2008].
38. Haslauer E. *Technol. Stud.* 2007; **4**: 123.
39. Cesareo R, Cappio Borlino C, Stara G, Brunetti A, Castallano A, Buccolieri G, Marabelli M, Giovagnolia AM, Gorghinian A, Gigante GE. *J. Trace Microprobe Tech.* 2000; **18**(1): 23.
40. Diana M, Gabrielli N, Ridolfi S. *X-Ray Spectrom.* 2007; **36**: 424.
41. Pilosi L (ed.). *Glass and Ceramics Conservation 2007*. Grafica Soca: Nova Gorica, Slovenia, 2007.
42. Müller W (ed). *BAM Forschungsbericht 215*, Verlag für neue Wissenschaften GmbH, Bremerhaven: Berlin 1995.
43. Pilz M. Fraunhofer ISC Jahresbericht 1997, 1997; 69.
44. Bernhardt R, Kruschke D. Restauro 6, 2000; 433.